Supplementary Information

Stretchable and Self-healing Electronic Skin Based on Piezoelectric/Triboelectric Polyester Elastomer for Deep and Superficial Sensation

Yanxiu Qiao[a, d], *Qian Zhang*[a, d], *Yong Xiang*[a, d], *Zhao Wang*[b,c *], *and Xiaoran Hu*[a,d *]

[a] School of Materials and Energy, University of Electronic Science and Technology of China, Chengdu, China
[b] Institute of Emergent Elastomers, School of Materials Science and Engineering, South China University of Technology, Guangzhou 510640, China
[c] State Key Laboratory of Organic-Inorganic Composites, Beijing University of Chemical Technology, Beijing 100029, P. R. China
[d] Chengdu CoreUnion Technology Co., Ltd
[*](Correspondence to Xiaoran Hu, e-mail:Huxiaoran@uestc.edu.cn)

Nuclear Magnetic Resonance

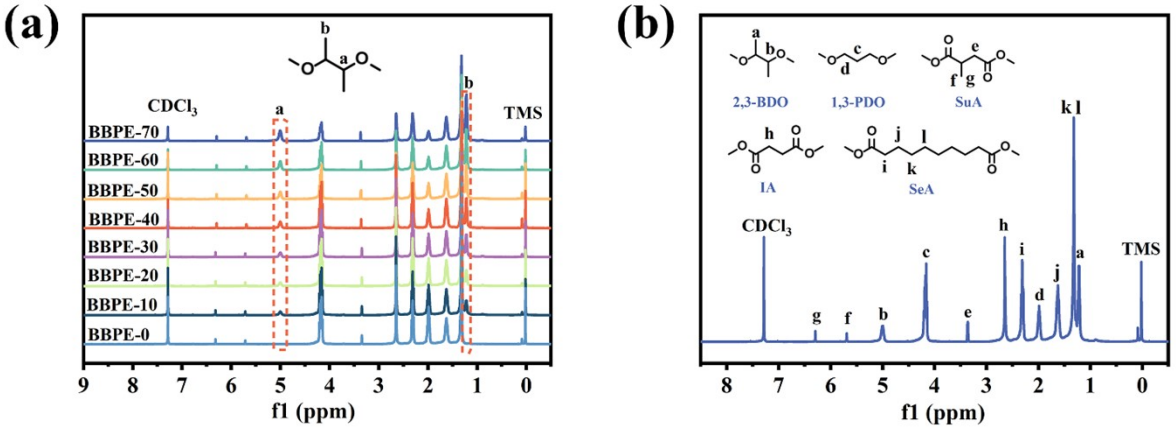

Figure S1. (a) [1]HNMR spectra of the BBPE copolyester series; (b) [1]HNMR spectra of the BBPE-50 copolyester

The compositions of BBPE are verified by [1]HNMR. All proton signals of the BBPE's repeating units are detected at their anticipated chemical shift values with corresponding peaks. A representative [1]H-NMR spectrum of BBPE-50 is shown in Fig S1b. The signals of the methylene groups in sebacic acid -(C**H**$_2$)$_4$-C**H**$_2$-C**H**$_2$-COO- are found at δ1.32(k\l), 1.62(j), and 2.32(i) ppm. The peaks at δ2.64(e) ppm originate from the protons of succinic acid -COO-(C**H**$_2$)$_2$-. The peaks at δ6.35(h),5.73(g) and 3.36(f) ppm are attributed to alkene and methylene group of itaconic acid -CO-C(=C**H**$_2$)-C**H**$_2$-. The presence of 1,3-propanediol -(C**H**$_2$)-C**H**$_2$-O- is confirmed by the peaks at δ1.98(d)

and 4.17(c) ppm. The peaks at δ1.22(a) and 5.01(b) ppm are attributed to methyl and methyne group of 2,3-butanediol -O-C**H**($C\mathbf{H}_3$)-. These two peaks demonstrate the successful introduction of 2,3-BDO repeating units into BBPE chains. The relative intensity of the peaks corresponding to the 2,3-BDO segments increases with increasing initial feeding of 2,3-BDO, indicating that the content of 2,3-BDO in these elastomers increases with increasing initial feeding of 2,3-BDO.

Fourier Transform Infrared Spectroscopy (FTIR)

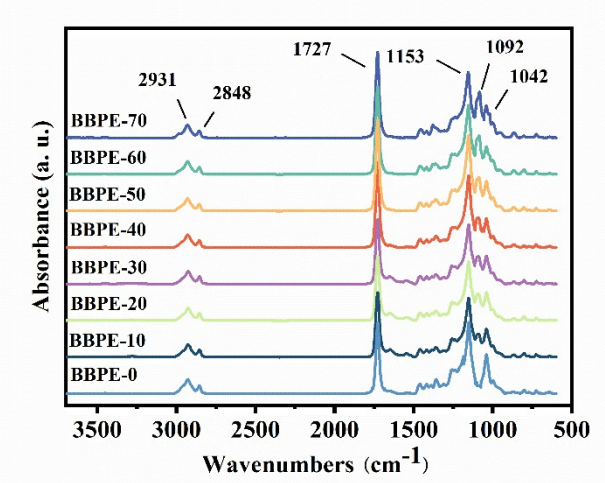

Figure S2. FTIR spectra of the BBPE copolyester series

Figure S2 shows the FTIR spectra of BBPE. The signal at 808 cm^{-1} is attributed to the presence of stretching and bending vibrations of -C=C-H from the double bonds in itaconate. The intense absorption at 1727 cm^{-1} is associated with the stretching vibration of the carbonyl group (C=O), indicating the formation of abundant ester bonds. The absorption at 1153 cm^{-1} confirms the presence of the C-O-C=O groups in ester bonds. The absorptions at 2931 cm^{-1} and 2848 cm^{-1} are assigned to the symmetric and the anti-symmetric stretching vibrations of methylene (-CH_2), respectively. The characteristic absorption observed at 1092cm^{-1} demonstrates the presence of C–O groups in the primary alcohol of 2,3-BDO, and the relative intensity of this absorption significantly increases with increasing content of 2,3-BDO, which is in accordance with the ^{1}HNMR results. These results confirm the successful introduction of 2,3-BDO into the macromolecular chains of the BBPE.

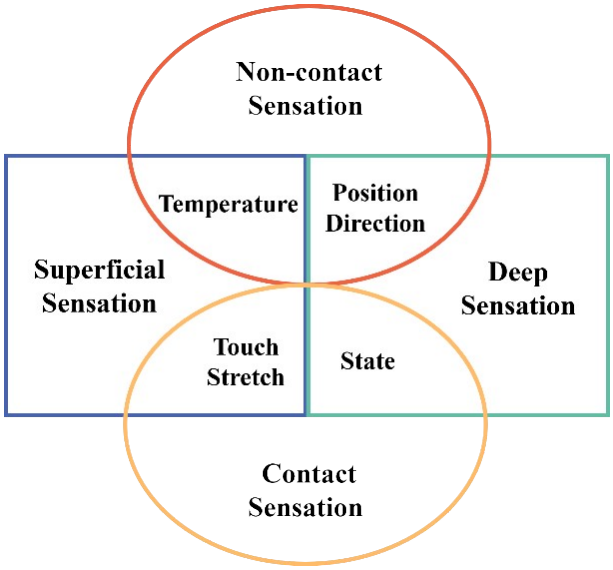

Figure S3. The relationship diagram of superficial sensation and deep sensation, as well as non-contact sensation and contact sensation

Deep sensation and superficial sensation are inherently segregated based on their definitions, while contact sensation and non-contact sensation exhibit non-intersecting domains according to whether physical contact occurs. Further subdivision of deep and superficial sensations leads us to broadly deduce the relationship diagram depicted above, albeit representing only a subset of the interconnections. Position and direction sensation within deep sensation, as well as temperature sensation within superficial sensations, are attributed to non-contact sensation. Conversely, state sensation within deep sensation and touch along with stretch within superficial sensation are categorized under the contact sensation. It is noteworthy that the realization of both deep and superficial sensations encompasses intricate varieties and mechanisms, with our research efforts focusing on a partial exploration thereof.

Mechanical property

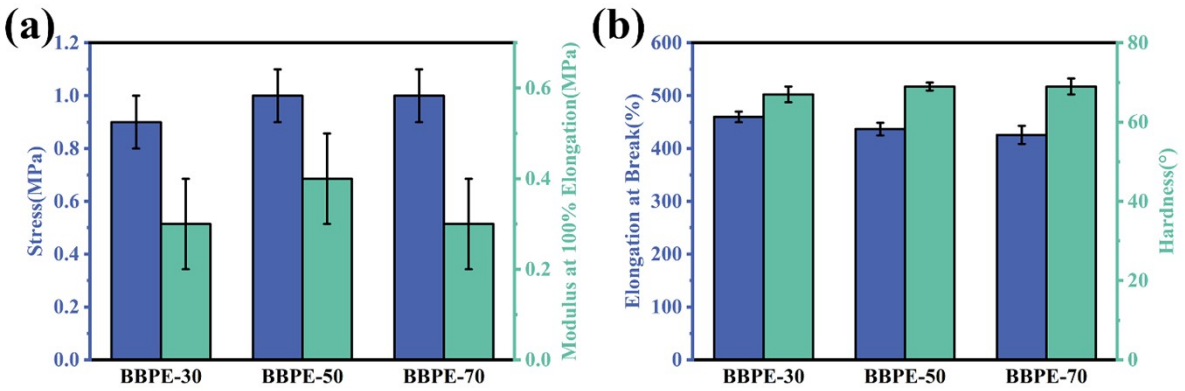

Figure S4. Mechanical properties of the BBPE copolyester series.

Piezoelectric and triboelectric properties

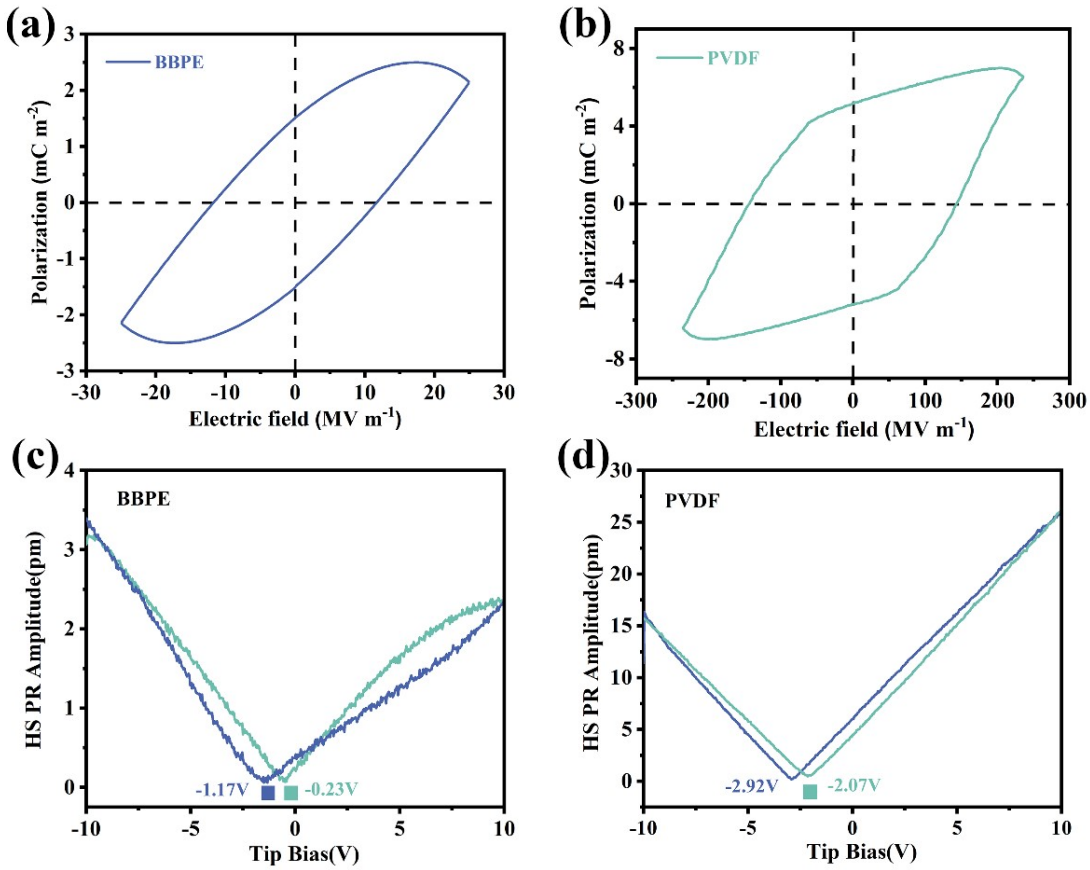

Figure S5. The P-E curves of (a) BBPE and (b) PVDF; The amplitude curve (butterfly curve) of (c) BBPE and (d) PVDF.

The P-E curves are obtained at 2 kV with BBPE thickness of 80 μm and the purchased PVDF thickness of 8.5 μm, respectively. As presented in Figure S1(a) and (b) ,the BBPE shows elliptical P-E curves due to possible large leakage current. The Pr value of 1.6 mC/m^2 is obtained with coercive electric field of 13 MV/m. The PVDF shows obvious higher coercive electric field of 240 MV/m and larger Pr value of 7.3 mC/m^2 compared with those of BBPE.

Furthermore, the clearly hysteresis can be observed in amplitude curve of BBPE from PFM methods, the strain mutation voltages are – 1.17 V and – 0.23 V, respectively (Figure S1(c)), while , the strain mutation voltages of PVDF are – 2.92 V and – 2.07 V(Figure S1(d)). Since the center of the amplitude curve does not coincide with 0 V, it indicates that the internal electric field can be formed in BBPE and PVDF, which is a solid description of its piezoelectric characteristics.

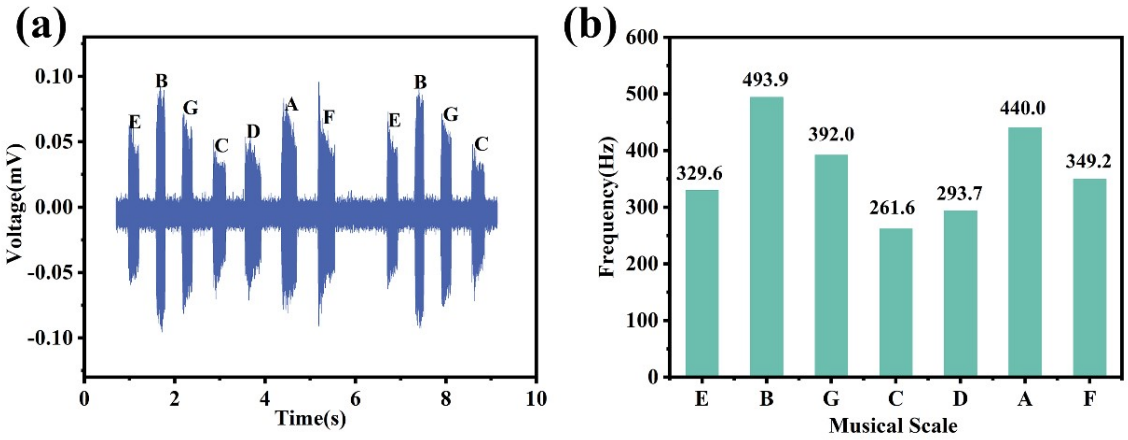

Figure S6. (a) Piezoelectric voltage behaviors of PBES under different musical scales.(b) The frequency diagram corresponding to different musical scales.

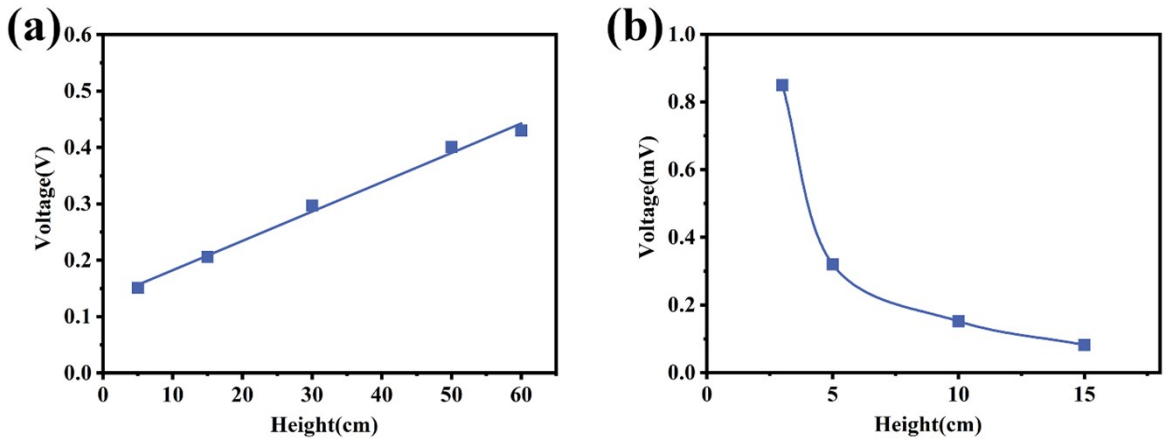

Figure S7. (a)Piezoelectric responses of PBES to different height of free-fall dropping; (b)Triboelectric responses of PBES to different height of PE film moving above.

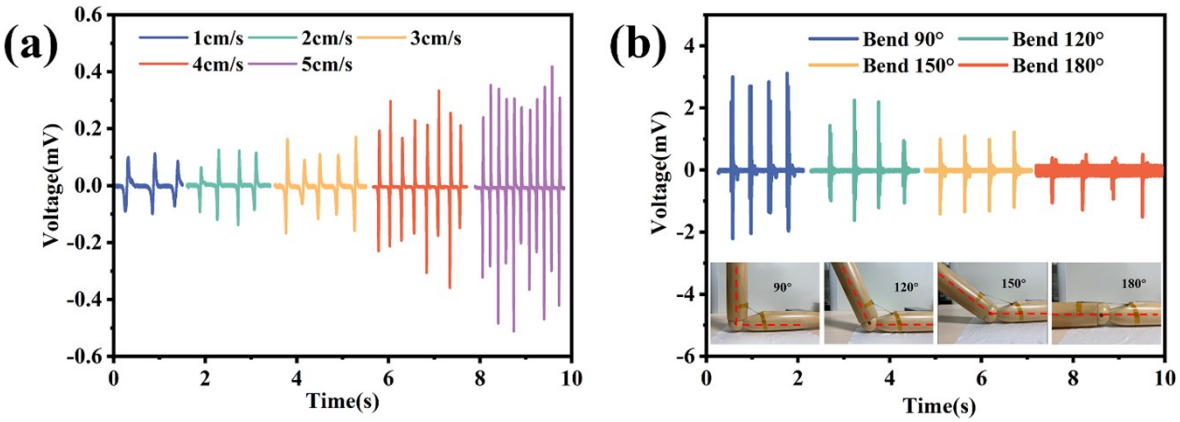

Figure S8. (a) Triboelectric open-circuit voltage behaviors of PBES to different speed of PE film moving above. (b) Piezoelectric open-circuit voltage behaviors of PBES to arm module bending at different angles.

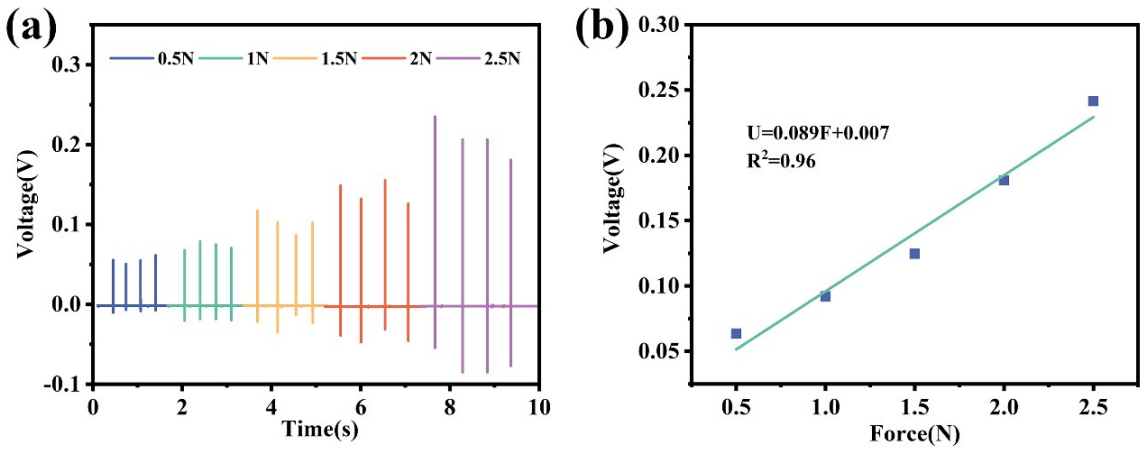

Figure S9. (a) Piezoelectric voltage behaviors of PBES under different force; (b) Linear fitting relationship between piezoelectric voltage and input force.

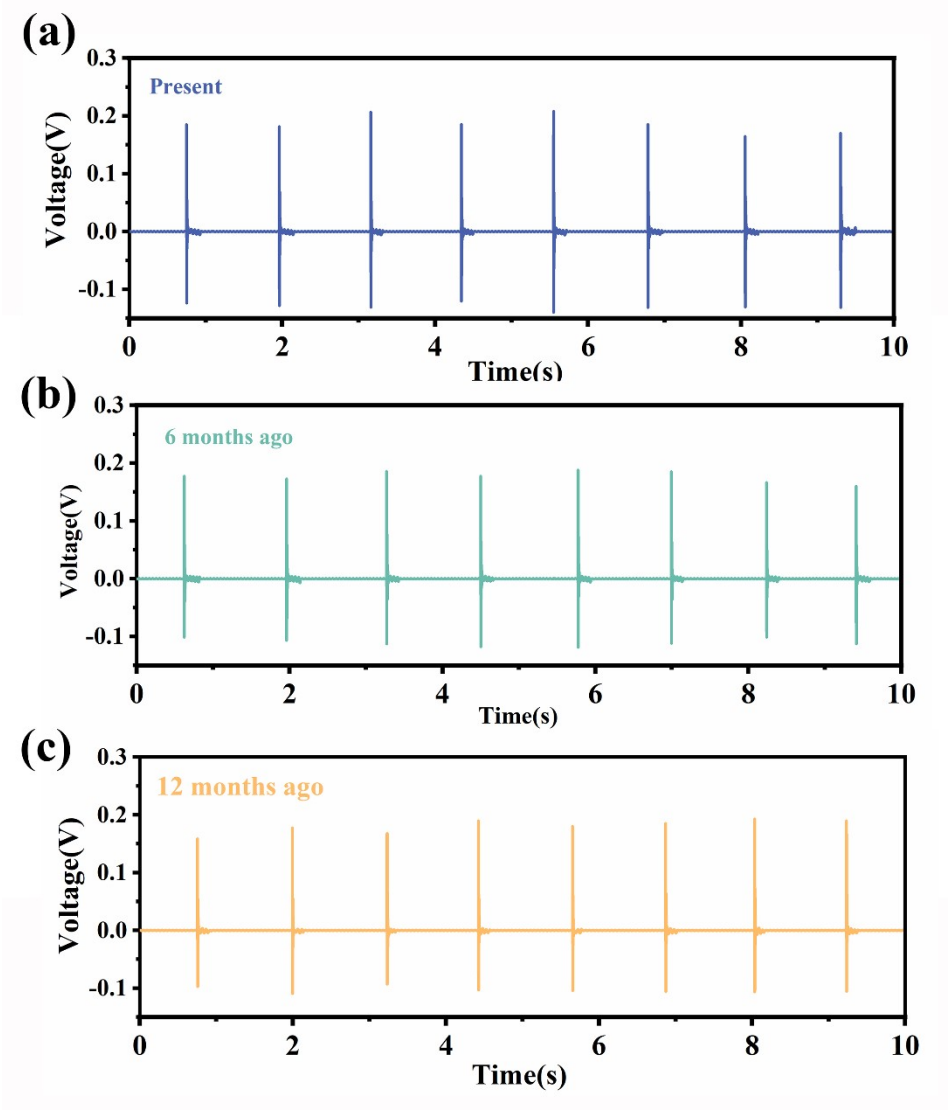

Figure S10. Piezoelectric voltage behaviors of PBES at different time.

Table S1. Piezoelectric responses of PBES at different time.

Preparation time	Voltage (mV)	Voltage retention rate(%)
Present	0.313±0.017	100.00
6 months ago	0.287±0.014	91.55
12 months ago	0.281±0.014	89.55

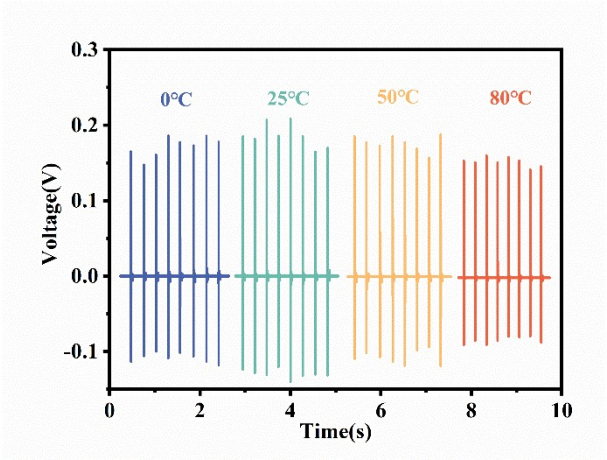

Figure S11. Piezoelectric voltage behaviors of PBES at different temperatures.

Table S2. Piezoelectric responses of PBES at different temperatures.

Temperature(℃)	Voltage (mV)	Voltage retention rate(%)
0	0.284±0.016	90.73
25	0.313±0.014	100.00
50	0.287±0.018	91.69
80	0.249±0.009	79.55

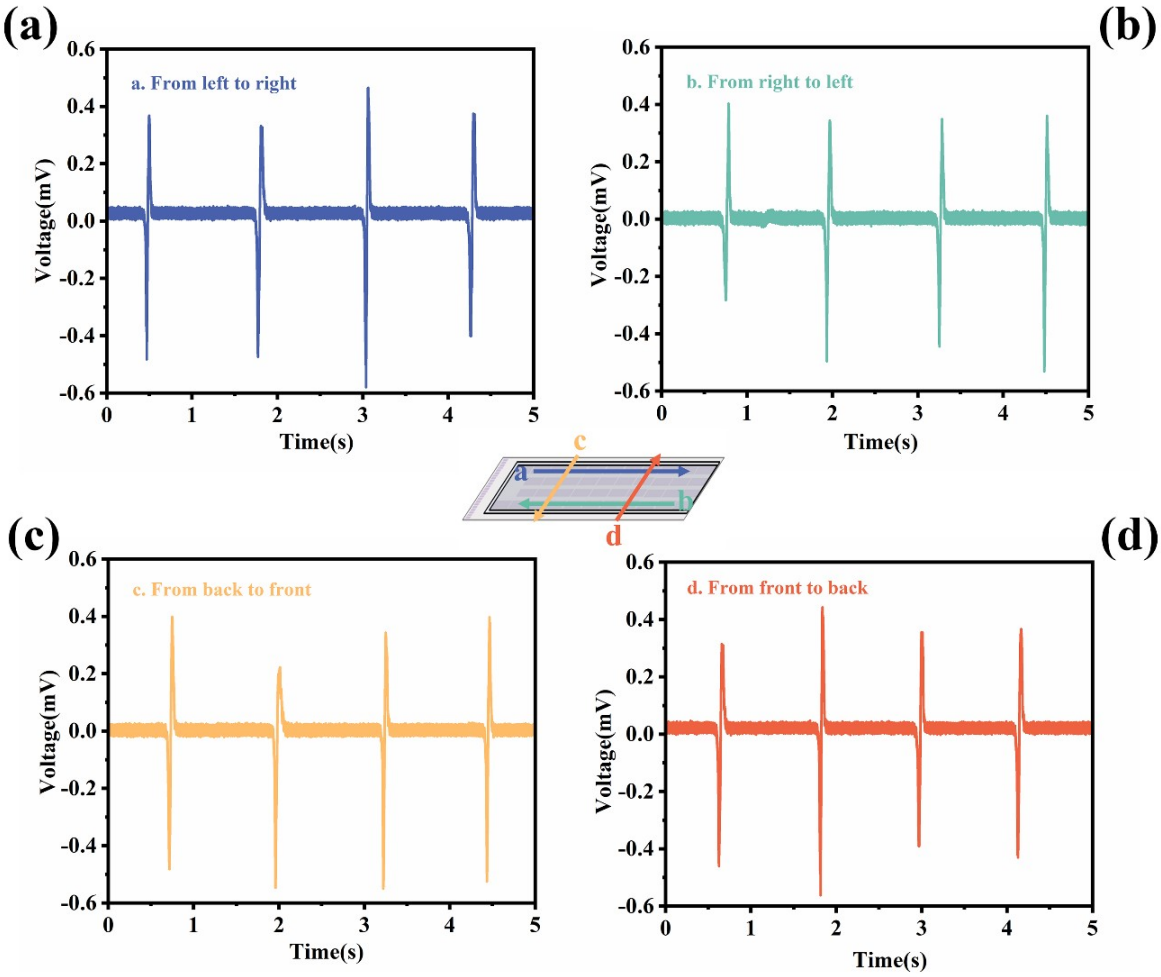

Figure S12. Triboelectric voltage behaviors of PE film in different motion directions above the PBES device.

Biocompatibility

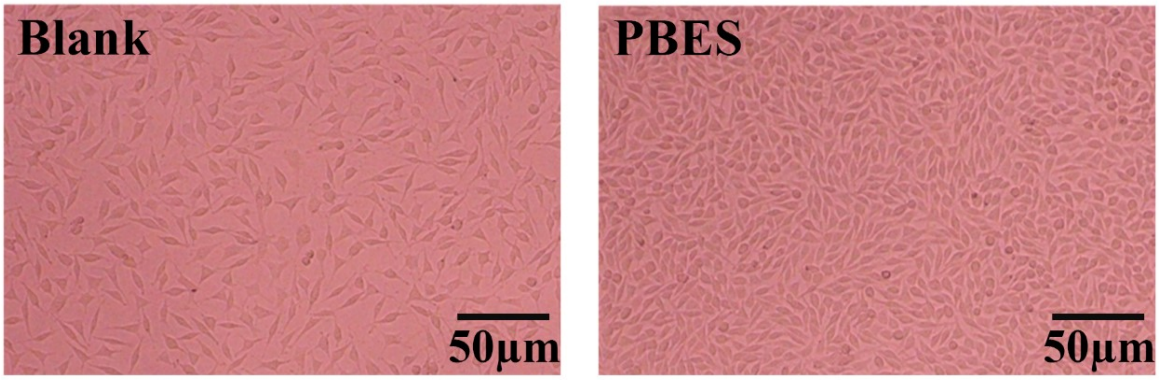

Figure S13. Optical image of L929 cells incubated for 3 days on the control sample and BBPE.

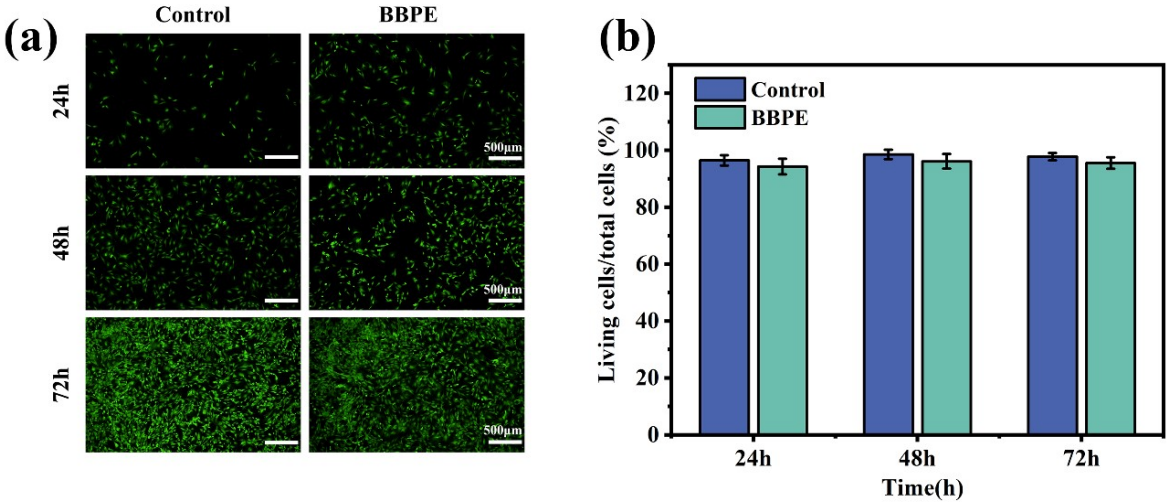

Figure S14. (a) Dead and live assay evaluation of tenocytes (green, live; red, dead) proliferation in normal medium and BBPE at 24, 48 and 72 hours. (b) The percentage of living cells in normal medium and BBPE.

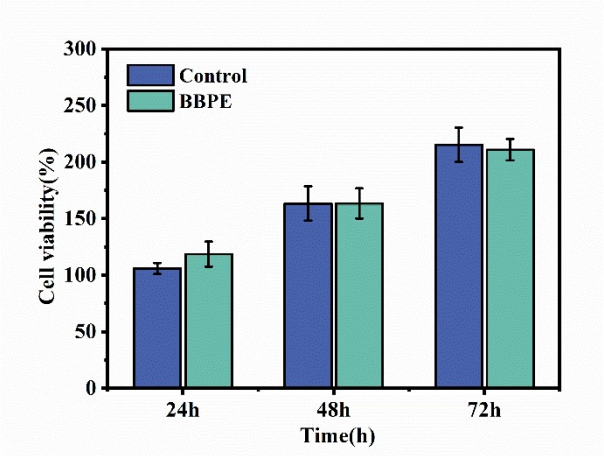

Figure S15. The cell viability of tenocytes cultured in normal medium and BBPE detected by CCK-8 assay.

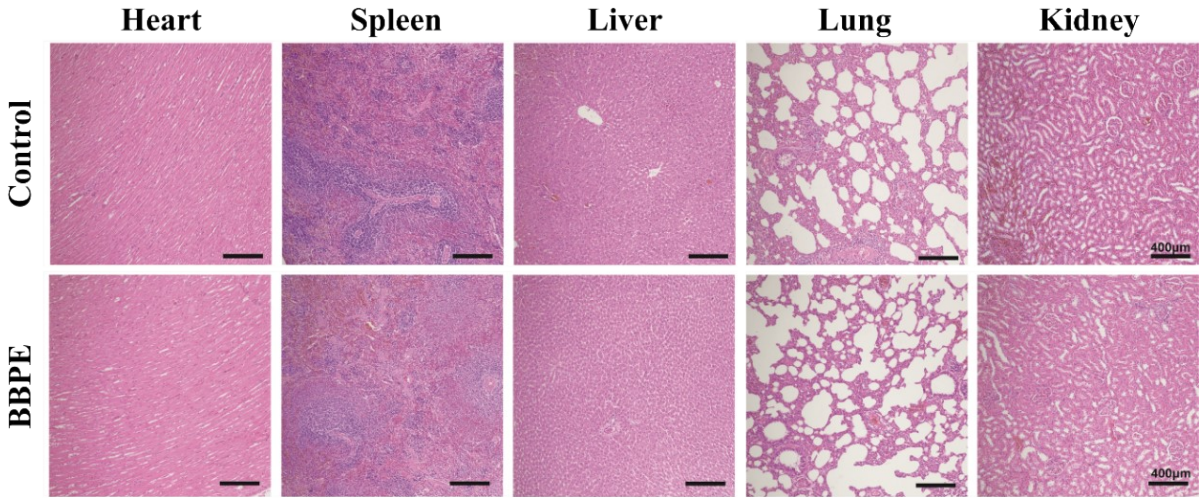

Figure S16. Biological toxicity validation of BBPE in vivo after 2 weeks treatment.

Self-healing properties

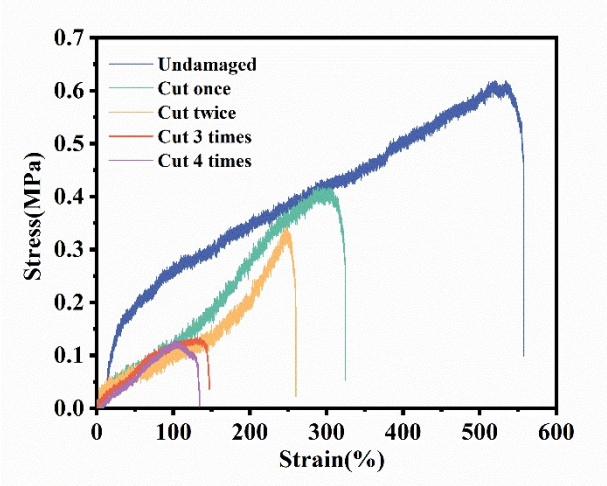

Figure S17. The mechanical properties of PBES generated after various cut-heal cycles.

Table S3. The mechanical properties of PBES after different cut-heal cycles.

Cut-heal cycles	Maximum Stress (MPa)	Elongation at Break (%)
0	0.6122±0.0012	557.54±3.24
1	0.4178±0.0023	324.78±2.56
2	0.3418±0.0015	259.69±4.11
3	0.1307±0.0029	147.01±2.81
4	0.1254±0.0008	132.48±3.29

Table S4. The abbreviations of proper nouns in the manuscript.

Abbreviation	Full Name
BBPE	Butanediol-based piezoelectric elastomer
PBES	Polyester-based electronic skin
BDO	Butanediol
PDO	Propanediol
SuA	Succinic Acid
SeA	Sebacic acid
IA	Itaconic Acid
DCP	Dicumyl peroxide
TBT	Tetrabutyl titanate
PE	Polyethylene
^{1}HNMR	Proton nuclear magnetic resonance
FTIR	Fourier transform infrared spectroscopy
DSC	Differential scanning calorimetry
XRD	X-ray diffraction
RGR	Relative growth rate

Table S5. Piezoelectric responses of PBES stretched to different length.

Length (cm)	Elongation (%)	Voltage (mV)
5	150	4.627
10	400	4.232
15	650	1.313
20	900	1.012

Table S6. Piezoelectric responses of PBES after different stretch-recovery cycles.

Stretch-recovery cycles.	Voltage (mV)	Voltage retention rate(%)
0	5.037	0
30	4.742	94.14
60	4.587	91.07
100	3.806	75.56

Table S7. Triboelectric responses of PBES to different area of PE film moving.

Area (cm^2)	Voltage (mV)
20×20	0.955
30×30	1.277
40×40	1.838
50×50	5.087

Table S8. Piezoelectric responses of PBES to finger bending at different angles.

Angle (°)	Voltage (mV)
180	0.097
150	0.278
120	0.362
90	0.521

Table S9. Piezoelectric responses of PBES after different cut-heal cycles.

Cut-heal cycles	Voltage (mV)	Voltage retention rate(%)
0	50.40	0
1	45.91	91.09
2	44.90	89.09
3	44.05	87.40
4	38.98	77.34